AGU ADVANCING EARTH AND SPACE SCIENCE

Water Resources Research

RESEARCH ARTICLE
10.1029/2022WR034266

On the Capabilities of Emerging Nonintrusive Methods to Estimate Bedform Characteristics and Bedload Rates

M. Muste[1], H. You[2], D. Kim[3], G. Fleit[4,5,6], S. Baranya[4,5], R. Tsubaki[7], D. Abraham[8], T. O. McAlpin[8], and K. E. Jones[8]

[1]Department of Civil and Environmental Engineering, IIHR-Hydroscience & Engineering, The University of Iowa, Iowa City, IA, USA, [2]K-water Research Institutes, Daejeon, South Korea, [3]Department of Civil & Environmental Engineering, Dankook University, Yongin, Korea, [4]Department of Hydraulic and Water Resources Engineering, Faculty of Civil Engineering, Budapest University of Technology and Economics, Budapest, Hungary, [5]Faculty of Civil Engineering, National Laboratory for Water Science and Water Security, Budapest University of Technology and Economics, Budapest, Hungary, [6]ELKH-BME Water Management Research Group, Budapest University of Technology and Economics, Budapest, Hungary, [7]Department of Civil Engineering, Hydraulic Engineering Laboratory, Nagoya University, Nagoya, Japan, [8]Coastal and Hydraulics Laboratory, U.S. Army Engineer Research and Development Center, Vicksburg, MS, USA

Key Points:

- Demonstrate Acoustic Mapping Velocimetry (AMV) feasibility for in-situ measurements bedform dynamics
- Identify sources of uncertainty in the AMV workflow subcomponents
- AMV characterization of bedform morpho-dynamics is within 22% of the estimates made with two other non-intrusive methods

Correspondence to:

H. You,
yhj87@hyrslab.com

Citation:

Muste, M., You, H., Kim, D., Fleit, G., Baranya, S., Tsubaki, R., et al. (2023). On the capabilities of emerging nonintrusive methods to estimate bedform characteristics and bedload rates. *Water Resources Research*, *59*, e2022WR034266. https://doi.org/10.1029/2022WR034266

Received 7 DEC 2022
Accepted 6 JUN 2023

Abstract A new measurement protocol, labeled Acoustic Mapping Velocimetry (AMV), has been successfully tested for in-situ estimation of bedload transport features in sandy beds. The AMV has proven efficient in using the dune-tracking method (DTM) for characterizing the bedform geometry and dynamics as well as for estimation of the rates of bedload transport. Given the novelty of the AMV protocol and its extensive reliance on multiple site-specific assumptions and user-defined parameters, a comparison of this emerging technique with other three non-intrusive DTM-based methods and analytical predictors is attempted in this paper. The comparison highlights that the AMV estimates are within 22% of the estimates with the other non-intrusive protocols and up to 98% different from analytical predictions. The observed differences are related to the possible sources of uncertainty in the AMV workflows and to the means to reduce their impact on the targeted estimations.

1. Introduction

The last four decades has brought a plethora of non-intrusive instruments for in-situ measurements of bed morphology dynamics, with most of them being highly efficient and operationally safe for the instruments and users. More importantly, the instruments acquire data with high sampling rates over a wide range of spatial and temporal scales. The superior capabilities of this new generation of instruments have produced considerable impacts on the in-situ quantification of bedload migration, an area that is considerably lagging the measurement capabilities available for other riverine hydro-morphodynamic processes (e.g., Gray et al., 2010). Among the new instruments in this area are those based on acoustic sensors (e.g., Thorne, 2014), tracer particles (e.g., Wilcock, 1997), and impact sensors (e.g., Reid et al., 1980). Comprehensive reviews of these instruments are offered by Ergenzinger and De Jong (2003) and Marquis and Roy (2012). Given that most of these instruments are new, they require adequate evaluation before applying them with high confidence in any measurement environment (Ancey, 2020; Le Guern et al., 2021). This paper is an effort along these lines.

In this paper, our attention is directed toward acoustic sensors, a family of instruments that marked a considerable progress in riverine measurement environments. Among the instruments from this category are the Acoustic Doppler Current Profilers (ADCP) (e.g., Conevski et al., 2020; Holmes, 2010; Rennie & Millar, 2004) and the single- or multi-beam echo-sounders (MBES) (Knaapen, 2004; Leary & Buscombe, 2020). Especially attractive for the measurement of bedform dynamics are the MBES because they produce two-dimensional (2-D) high-resolution maps with high efficiency (Aberle et al., 2012; Abraham & Kuhnle, 2006; Dinehart, 2002; Duffy, 2006). Using topographic maps acquired with MBES, one can obtain bedload transport rates using the "inverse," or the morphologic approach, whereby direct observations of the changes in channel morphology over time are used to infer rates of sediment transport (Ashmore & Church, 1998). The morphological approach term was introduced to distinguish it from the "forward" methods that determine the resultant bedforms from governing equations driving the bedload transport rates. We define herein bedload transport rate as a local, mean value to distinguish it from bedload discharge representing a cross-sectional transport rate (Gomez, 1991).

Among the emerging measurement protocols for investigating bedform transport is the dune-tracking method (DTM) applied to repeated MBES surveys (Duffy, 2006; Vericat et al., 2017). The DTM is considered as one of the most accurate method for estimation of bedload rates in sand-bedded rivers (Leary & Buscombe, 2020). The DTM enables not only exploration of erosion and deposition spatial patterns but also a robust procedure for estimating bedform transport rates over a wide range of spatio-temporal scales. There are two groups of DTM approaches for estimation of the bedload transport rates from MBES surveys. The first group determines the bedform migration velocity using Particle Image Velocimetry (PIV) principles (e.g., Duffy, 2006; Knaapen et al., 2005). The second group determines the bedform volumetric changes caused by dune migration (e.g., Abraham et al., 2011; Nittrouer et al., 2008). In this paper we focus on the strengths and limitations of the PIV group as embodied in the Acoustic Mapping Velocimetry (AMV) developed at IIHR-Hydroscience & Engineering (IIHR) first described in Muste et al. (2016). Given the lack of a widely-recognized "reference" method for validating in-situ bedload discharge measurements, a natural choice for its evaluation is the Integrated Section Surface Difference Over Time, version 2 method (ISSDOTv2) based on tracking dune volumetric changes developed by US Army Corps of Engineers (USACE) (McAlpin et al., 2022). The AMV and ISSDOTv2 are based on governing equations developed by Exner (1931). The second method uses refinements introduced by Abraham et al. (2011) and Simons et al. (1965).

The AMV concept was first proof-tested through laboratory experiments where its validation was successfully carried out using conventional bedload measurement approaches (Muste et al., 2016). Soon thereafter, a preliminary study was carried out to test the AMV capabilities for estimating bedload transport rates in-situ (Baranya et al., 2016). More recently, two other studies have investigated optimizations of various AMV aspects relevant to bedload transport: evaluation of the IV approaches for AMV (You, Kim, et al., 2021) and formulation of practical guidance for data acquisition to adequately capture the bedform dynamics in natural rivers (You, Muste, et al., 2021). This paper is the first attempt to evaluate the AMV performance for in-situ estimation of the bedform transport discharge as originally proposed in Muste et al. (2019). The discussion in this paper assumes that the bedforms are mostly sandy, quasi-unidirectional, fully developed, and in equilibrium (i.e., the geometry and dynamics remain quasi-constant with flow strength change).

The paper describes first the AMV workflow for in-situ estimation of the bedload transport rates along with criteria for selecting the ancillary parameters. A pseudo AMV validation is subsequently attempted by comparing two AMV alternatives with ISSDOTv2 bedload discharge estimates and with predictions obtained with "forward" analytical methods for bedload transport rate estimation. We use the "pseudo" qualifier to highlight that this area of science lacks a reference methodology and it is notorious for evaluations that differ up to an order of magnitude in the results (Ancey, 2020). The Discussion section compares the above methods along with preliminary inferences on the differences in the results. The main contribution of this paper is to better inform users on the impact of user-selected parameters on the estimation of bedload transport rates and discharges with DTM-based methods.

2. AMV Procedures and Associated Parameters

The AMV procedures for quantifying the much-needed bedload rates entail a combination of concepts and processing techniques used for acoustic mapping and image velocimetry (IV). The unique advantage of the AMV method is that it reveals simultaneously both the bedform geometry as well as the two-dimensional velocity vector field using the same set of raw measurements (Baranya et al., 2022). The AMV principle for estimating the bedform migration rate is based on the concept of tracking a triangular-shaped bedform moving in the streamwise direction. The terms bedform and dune are interchangeably used herein. AMV protocols analyze first the bedform patterns to determine a representative bedform geometry. Subsequently, the dynamics of the bedforms is determined from a sequence of acoustic maps taken at short time intervals. The AMV workflow is summarized in Figure 1 and Table 1. Figure 1 visualizes the workflow while Table 1 provides details for each sequence including the potential sources of uncertainty. The steps in Figure 1 are illustrated with data from the case study analyzed in Section 3. Table 1 groups the workflow steps per type of activity, that is, data acquisition and data processing, to highlight that most of the user-selected parameters pertain to data processing. The two summaries often make reference to the companion AMV papers dealing with the performance of various IV approaches (You, Kim, et al., 2021) and with guidelines for AMV in-situ implementation (You, Muste, et al., 2021).

The first AMV workflow step is the creation of the acoustic maps as a continuous depth-data layer covering the targeted area on the channel bottom. River management agencies regularly acquire such maps to document bedform characteristics and their distribution across river cross-sections and reaches (Ramirez et al., 2018). There

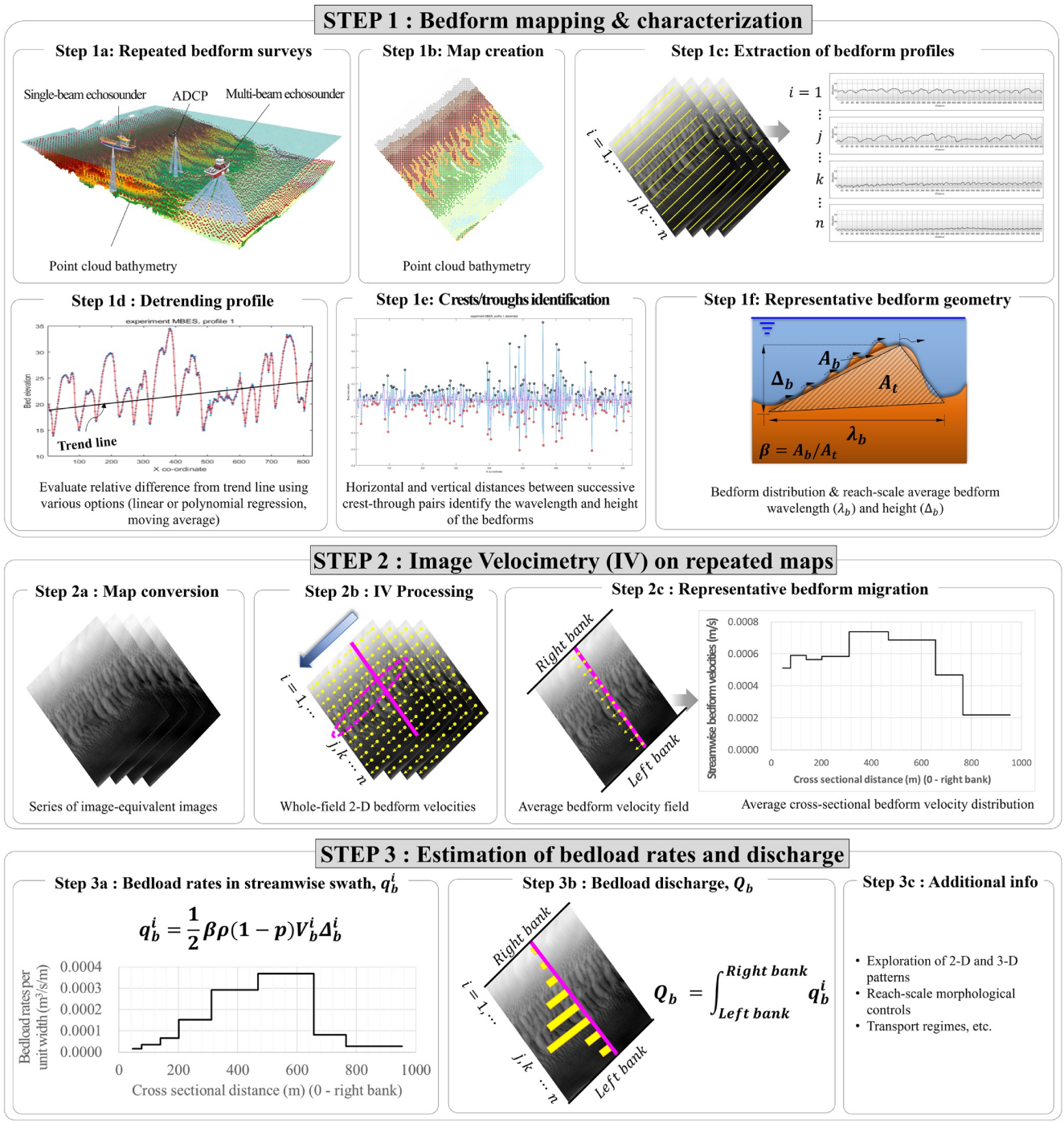

Figure 1. Flowchart of the acoustic mapping velocimetry (AMV) protocol for the estimation of the bedload transport discharge.

are multiple instruments for non-intrusively obtaining bathymetric maps (see Figure 1, Step 1a). The accuracy of the captured bedforms is controlled by the MBES sounding density which in turn depends on the instrument footprint size, pinging rate, as well as on the vessel speed and the local water depth (You, Muste, et al., 2021). Given the efficiency of the MBES measurements, the river bottom can be surveyed relatively quickly over large bed area. The MBES measurements presented in this study are acquired in successive swaths aligned in the streamwise direction. The surveyed swaths are conditioned and aggregated in Step 1b in the form of a map. The bedform profiles and their distribution along any planar direction are extracted from the assembled acoustic maps

Water Resources Research

10.1029/2022WR034266

Table 1
Step-By-Step Acoustic Mapping Velocimetry Procedures Used in the Present Study for Estimation of the Bedload Transport Discharge

AMV protocol step & outcomes		Data acquisition & processing: Protocol/algorithm	Data acquisition & processing: Parameters	Uncertainty source (relevant info)
In-situ data acquisition				
Step 1a: Repeated bedform surveys	Individual acoustic maps	Bedform sounding	• A priori information on reach-scale bedform characteristics & distribution	1. Instrument spatial resolution (Wilbers, 2004)
				2. Instrument sampling rate (Wilbers, 2004)
			• Water depth and its reach-scale distribution	3. Across-beam spacing (Duffy, 2006)
				4. Total mapping duration (Muste et al., 2016)
			• Number of bedform wavelengths within mapped area	5. Navigation pattern & vessel speed (Duffy, 2006; Wilbers, 2004)
				6. Measurement environment (Duffy, 2006)
	Series of multiple maps	Repeated soundings	• Time interval between consecutive maps versus bedform migration velocity	7. Size of the mapped area (You, Muste, et al., 2021)
Data processing				8. Navigation patterns & vessel speed (Duffy, 2006; You, Muste, et al., 2021)
Steps 1b and 1c: Map creation & extraction of the bedform profiles	Contiguous 3-D map	• Raw data conditioning (?)	• Density of the grid for interpolation	9. Pre-processing (Tsubaki et al., 2012)
		• Interpolation of depth cloud points • Rasterization	• User-specified parameters for interpolation	10. Interpolation procedure algorithm & user-parameter settings (Kemp, 1993)
Steps 1d, 1e, and 1e: Determination of the representative bedform geometry	Average bedform wavelength (λ), height (Δ), and shape factor (β)	Bedform Tracking Tool (BTT)	• Selection of the cross-sectional sub-sections used for analysis	11. Number of sub-sections for bedform characterization (You, Muste, et al., 2021)
			• Trend line for regression	12. # of dune wavelengths within the mapped area (Le Guern et al., 2021)
			• Built-in-checking parameters	13. Number of images used for bedform characterization (You, Muste, et al., 2021)
				14. BTT parameter selection (Van der Mark et al., 2008)
Step 2a: Map conversion	Gray-level images	Conversion of color-coded to 256 gray-level images	• Resolution of the pixel image	15. Selection of the pixel size (Baranya et al., 2022)
			• Image conditioning (e.g., bilinear interpolation)	16. Image size (You, Muste, et al., 2021)
			• Normalization parameter (NAVD-88)	17. Interpolation

Water Resources Research

10.1029/2022WR034266

Table 1
Continued

AMV protocol step & outcomes		Data acquisition & processing: Protocol/algorithm	Data acquisition & processing: Parameters	Uncertainty source (relevant info)
Step 2b: Image velocimetry (IV) processing	Whole-field 2-D bedform velocity field & sectional distributions	• Conventional Cross-Correlation (CCM)	• Interrogation area (all methods)	18. Choice of IV protocol selection (You, Kim, et al., 2021)
		• Optical Flow (OF)	• Image partitioning per velocity sub-fields (CCM)	19. Interrogation area selection—all methods—(You, Kim, et al., 2021)
		• High-Gradient Pattern IV (HGPIV)	• Search area (CCM)	20. Number of sub-areas & search window size—CCM—(You, Kim, et al., 2021)
			• Grid density (all methods)	21. Number & timing for the repeated maps—all methods—(You, Muste, et al., 2021)
Step 2c: Representative bedform dynamics	Average bedform migration velocity	Statistics applied to the whole-field bedform velocities	• Selection of cross-sectional sub-sections used for analysis	22. Number of sub-sections for bedform characterization (You, Muste, et al., 2021)
				23. Number of bedform wavelengths within the mapped area (Le Guern et al., 2021)
				24. Number of images used for bedform characterization (You, Muste, et al., 2021)
Step 3a: Bedload rates calculation in individual swaths	Distribution of the bedload rates	Exner equation (Exner, 1931; Simons et al., 1965) with proper consideration of superposed dunes (Wilbers, 2004)	• Bed material density, $\boldsymbol{\rho}$	25. Number of sub-sections for bedform characterization (You, Muste, et al., 2021)
			• Bedform average velocity, $\boldsymbol{V}_b^i$	26. Bedform velocity determination (Dillo, 1960)
			• Bedform average height, Δ_b^i	27. Bedform average height determination (Wilbers, 2004)
			• Bed material porosity, p	28. Porosity estimation (Le Guern et al., 2021)
			• Bedform shape factor, β	29. Shape factor estimation (Duffy, 2006)
Step 3b: Bedload discharge	Cross-sectional transport rate	Summation of bedload rates in individual swaths		30. Estimation of the bedload rates in the unmeasured areas near the banks

(Step 1c). For characterizing the bedform dynamics, repetition of such maps is needed at a rate commensurate with the bedform migration velocity (You, Muste, et al., 2021).

Steps 1d, 1e, and 1f convert the acoustic maps into a generalized representation of the bedforms over the surveyed reach. These steps are critical to ensure the reliability of the dune tracking. They lead to one representative dune for each subsection of the mapped area, characterized by a dune height (Δ) and length/wavelength (λ), as illustrated in Figure 1f. The dune height is the difference between the crest and trough of the dune while the dune wavelength is the distance between two subsequent crests or troughs. The accuracy of the estimates of the dune characteristics is more sensitive to the density of the measured points along a profile than on the method used to extract the dune characteristics from a profile (Wilbers, 2004). The optimal outcome of Step 1f is obtained if the bedform characteristic extraction is made along the same directions as those used in Step 1a for surveying the targeted area as this approach ensures a more accurate timing for the IV processing (You, Muste, et al., 2021). There are multiple approaches to quantify the average characteristics of the dune geometry (e.g., Bradley & Venditti, 2017; Cisneros et al., 2020; Gutierrez et al., 2018; Le Guern et al., 2021; Zomer et al., 2022) These procedures are based on various principles (from statistical to wavelet analysis) with the goal to automatically extract representative bedform heights and wavelengths. The AMV processing approaches developed so far use the Bedform Tracking Tool (BTT) illustrated in Steps 1d and 1e as developed by Van der Mark et al. (2008). The BTT protocol for bedform characteristics estimation is based on statistical techniques and geometric transformations that requires user-defined parameters that can drastically influence the processed output.

In Step 2 of the AMV workflow, the dune migration is quantified using procedures pertaining to IV processing. These procedures are applied to a series of acoustic maps obtained in Step 1b after their conversion to an image equivalent (Step 2a). While production of acoustic maps is quite mature, the issue of selecting the optimum data acquisition and processing protocols to accurately capture 2-D velocity fields associated with bedform migration in field conditions is still under scrutiny (Leary & Buscombe, 2020; You, Kim, et al., 2021). Steps 2b and 2c provide the dynamic characteristics for the representative bedform identified in Step 1c. For the present study, the execution of Steps 2b and 2c is made with the High-Gradient Pattern Image Velocimetry (HGPIV) approach developed by You, Kim, et al. (2021) and Cross-Correlation Method (CCM) developed by Baranya et al. (2022). Optimal AMV results are obtained when the rules of thumb associated with IV processing (Adrian, 1991; Detert, 2021; Raffel et al., 2007) are observed from early stages of acoustic map acquisition (You, Muste, et al., 2021). One important rule is to ensure a bedform moves no more than 80% or less than 20% of the representative dune wavelength in the time between repeated surveys. Another critical IV constraint is the selection of the IV approach that best fits the texture contained in the image-equivalent maps (You, Muste, et al., 2021).

Step 3 of the AMV implementation is based on the dune tracking model originally developed by Exner (1931) where it is assumed that the entire bedform cross-sectional area passes through a given point on the bed. The method is applied to the representative bedform identified in Step 1f under the assumption that it accurately represents the wave train contained in the longitudinal profile. The Exner model modified by Simons et al. (1965) entails further simplifications that do not explicitly account for the fact that dunes can take multiple forms depending on the local mean flow and turbulence characteristics as well as bulk parameters such as Froude number and bed sediment material (e.g., ASCE, 2008; Best, 2005, p. 82). In addition to the dune height, Δ, obtained from Step 1f and the migration velocity, U_b, determined from the in-situ acquired data in Step 2c, the Exner model entails the shape factor, β, and the porosity, p (see Step 3a). The shape factor, β, is related to the deviation of the representative bedform from the generally-accepted triangular shape (Duffy, 2006). According to Wilbers (2004) the shape factors can be expressed as $\beta = 2V/\lambda$, where V is the volume of bed form per unit width, λ is the bedform wavelength and it ranges between 1 and 1.51. Values for the porosity estimates range between 0.35 and 0.4 and can be found in various sources (Gibb et al., 1984; Le Guern et al., 2021; Wu & Wang, 2006). Selection of the model parameters needs to be judicious as their values can sensibly influence the estimated bedload rates.

Given the variability of the bedform geometry across the section, the above variables are most-often represented as cross-sectional distributions along streamwise-oriented swaths. In the present case study, the variation of the dune heights and lengths span over two magnitude orders (see Figure 1, Step 1c). This cross-stream variability might entail regions where secondary dunes are superposed on the primary ones over the entire dune wavelength or only on the stoss-side of the dunes. For the former case, there is a need to account for the presence of secondary dunes in the estimation of the bedload transport rates (Wilbers, 2004). Under the assumption that the moving bedforms maintain the volume balance between erosion on the stoss side and deposition of the lee side

of the bedform, the transport rates can be obtained as described in Step 3a, Figure 1 (Claude et al., 2012). For the MBES measurements analyzed herein, the superposed secondary dunes are mostly present on the stoss side of the primary dunes. It is also noted that all methods discussed in this paper captures the sediment moving as large primary dunes as well as the secondary dunes superimposed on the primary dunes. The bedload transport rate across the stream cross section (a.k.a. bedload discharge) is obtained in Step 3b through the summation of the rates estimated in individual swaths. The accuracy of the transport rates is commensurate with the proper characterization of the dimensionality of the bedforms (i.e., two- or three-dimensional) and the presence or absence of the superposed dunes. Given the high variability of the bedforms in natural rivers, most of the attention should be focused on the geometry and dynamics of the large-size bedforms as they dominate the overall bedload transport rate.

3. Case Study: AMV Applied to In-Situ MBES Measurements

The MBES measurements presented herein are an integral part of a comprehensive study conducted by the US Army Corps of Engineers (USACE) over extended spatial and temporal scales with the intent to provide calibration and validation data for developing numerical models focused on sediment transport processes (Ramirez et al., 2018). As illustrated in the legend of Figure 2, the comprehensive data acquisition campaigns include MBES surveys, measurement of suspended sediment (red dots), acquisition of ADCP data from fixed locations (FV ADCP) and transects (MV ADCP), sampling of bed material at selected locations (yellow squares), and water surface profiling over extended distances (450 km). A secondary goal of the study was to collect repeated bathymetric data for quantifying the bedload transport using the ISSDOTv2 methodology developed by Abraham et al. (2011) that eventually were used to determine a bedload rating curve for a wide range of flow conditions occurring at this location (Jones et al., 2018). Fortunately, the MBES measurements used for this study fulfill all the above IV rules of thumb despite not originally being collected with AMV implementation in mind. Actually the case study measurements are conservative by multiple accounts (You, Muste, et al., 2021).

The data for the MBES study were collected in the Mississippi River near Vicksburg during low- and high-flow conditions (see Figure 2a). The flow during the measurements were quasi-steady: for the 3 October 2012 low-flow event the stage varied about 2% and the discharge 1% while for the 29 April 2013 high-flow event the stage and discharge varied less than 1%. Approximately 3.2-km long MBES bathymetric measurements were collected for each flow condition near River Mile 433 to infer dune characteristics and their preferential pathways. Following the 3.2 km long reach inspection, smaller stream reach areas were identified where the MBES bathymetric surveys were repeated to provide the sequential maps required by the ISSDOTv2 method. The essential conditions for the two selected cases are presented in Figure 2 and Table 2. The bathymetric mapping was performed with MBES along longitudinal swaths utilizing a 500 KHz Geoswath multi-beam echo sounder (Ramirez et al., 2018). An RTK GPS was connected to the survey boat having a horizontal accuracy of ± 2 cm. The vertical resolution of bathymetric elevations was approximately 3 cm for 50-m water depth. In order to capture the displacement of the bedforms, the bed scanning was repeated for six and four times in low and high flows, respectively. The time between MBES repeated surveys in the two field campaigns was dictated by practical considerations. Basically, the MBES maps were acquired back-to-back after each cross-sectional scanning was finalized.

The bathymetric surveys for ISSDOTv2 measurements were obtained by aggregating MBES strips (swaths) surveyed sequentially in the streamwise direction (see Figures 3a and 3b). Note that one swath-length between 1 and 2 was lost in the data acquisition at the higher flowrate. The aggregated bank-to-bank surveys indicate large dunes in the center of the channel extending toward the right descending bank and smaller dune along the thalweg. Comparing the maps at the low and high flows, it can be noticed that overall the dune wavelengths for the lower flow are larger than for the larger flow. This morphing appears to be driven by secondary dunes translating over the primary, larger, dunes according to Ramirez et al. (2018). Along channel bedform profiles at the same location for both flowrates are illustrated in Figures 3c and 3d.

The AMV version presented in this section is labeled as AMV-IIHR (You, Kim, et al., 2021) to distinguish it from the AMV-BME (Baranya et al., 2022). The only distinction between these two AMV approaches is the IV processing algorithm (see Section 4). The average bedform height, bedform velocities, and the bedload transport rates per unit width (i.e., $kgs^{-1}m^{-1}$) are determined as described in Section 2. The estimation of the representative bedform geometry is made for each individual swath by first averaging across and then along the individual swath areas. We choose the above-mentioned approach to uniformly compare our AMV results with the other processing alternatives that used the same approach for averaging (see Section 4). The surveyed areas for the low and high flows

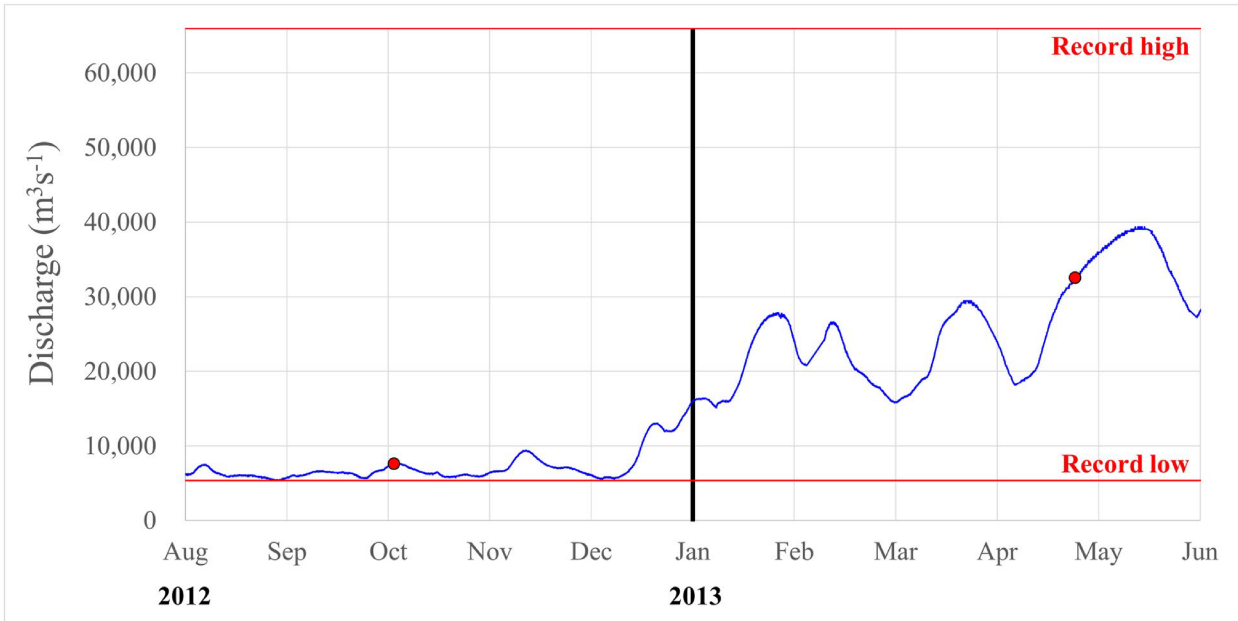

(a)

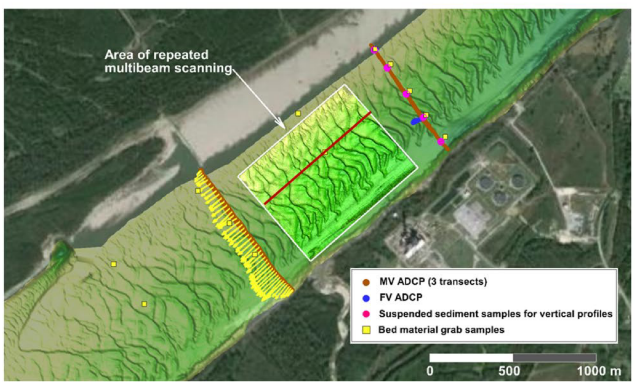

(b)

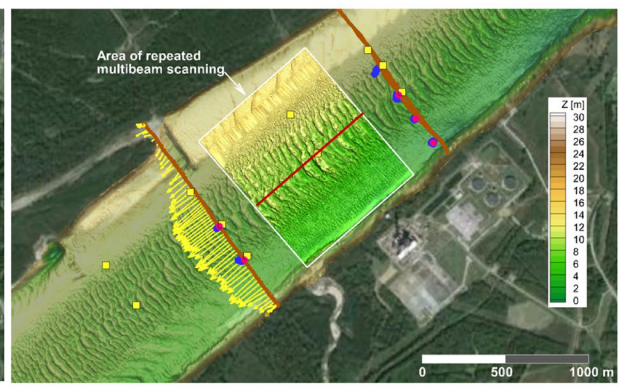

(c)

Figure 2. USACE multi-probe measurements in Mississippi River near Vicksburg (MS) entailing a section of the 3.2-km long Multi-Beam Echo-Sounders (MBES) surveys: (a) stage time series for the USACE Vicksburg (MS) gaging station located at River Mile 435.4 (data retrieved from: www.rivergages.com); The red dots on the plot indicate the time of the MBES surveys; (b) measurements acquired at low flow on 3 October 2012; and (c) measurements acquired at high flow on 29 April 2013.

contain 8 and 12 swaths, respectively. The results of these successive calculations are illustrated in Figures 4a and 4b, as distributions per swath width. The average height of the bedform geometry (Step 1c in Table 1) is determined using the BTT published by Van der Mark et al. (2008). The BTT procedure entails an automatized technique to extract statistical information on the characteristic average bedform heights and wavelengths, as well as the presence of superposed dunes. You, Kim, et al. (2021) and CCM developed by Baranya et al. (2022).

The bedform dynamics (Step 2b in Table 1) is obtained with the new HGPIV approach (You, Kim, et al., 2021). HGPIV combines the processing robustness of the conventional CCM with the computational efficiency of the optical flow method (OFM). The OFM is applied first to automatically determine the optimal search windows over the whole image area. Subsequently, CCM uses the OFM-determined search windows to locally resolve velocity fields associated with the pattern movement (You, Kim, et al., 2021). Given the high-density of the IV computational grid (You, Muste, et al., 2021), it is assumed that both the primary and secondary dunes are included in the calculation of the bedload transport rate. The bedform velocities are presented in Figures 4c and 4d as distributions of average

Table 2
Flow and Multi-Beam Echo-Sounders Characteristics for the Measurements Depicted in Figure 2

	Low flow (10 March 2012)	High flow (29 April 2013)
Discharge (m^3/s)	7,617	32,281
Channel width (m)	990	1,400
Active channel width (m)	560	900
Mean depth (m)	6.4	16
Mean flow velocity (m/s)	1.06	1.40
Bed material grain size, d_{50}, (mm)	0.4	0.4
Nr. of swaths	8	12
Length of swaths (m)	850	990
# of repeated scans	6	4
Average elapsed time between scans (hours)	0.1 (=6 min)	1.5

velocities over the entire area of the individual swaths measured during the two surveys. Finally, the bedload transport rates are estimated following Steps 3a and 3b in Table 1 by identically pairing the calculations for the representative bedform geometry and the average velocity for each swath. The values for the parameters used for the computation of bedform transport are: shape factor $\beta = 1.15$ (Wilbers, 2004), porosity $p = 0.381$ (determined for sediment with $d_{50} = 0.429$ mm as per Wu & Wang, 2006), and sediment density, ρ, set at 2,650 kgm^{-3}. To highlight the impact of the selection of the shape factor and porosity values within their recommended ranges, bounding intervals are determined using variability ranges found in literature for these parameters as illustrated in Figures 4g and 4h. The minimum and maximum bounds shown in these figures are for $\beta = 1$ and $p = 0.4$ and $\beta = 1.51$ and $p = 0.35$, respectively.

The capabilities of the AMV to capture bedform hydro-morphodynamic characteristics with high spatio-temporal resolution and over relatively large areas enable a wide range of unique inferences and analyses on the mechanisms of bedform dynamics and processes. While this paper is mostly focused on the measurement method evaluation rather than aspects of the sediment transport mechanics, we note several features of interest revealed in Figures 2 and 4. First, the large bedform front in the lower left corner of Figure 2b (indicating the change in flow regime) reveals that the equilibrium regime for the bedform transport is relatively short even if the flows are low and that the bedform characteristics respond swiftly to changes in the flow.

Other notable features are shown in Figures 4a and 4b, where can be observed that the dune heights are lower in the low-flow case than in the high-flow, and in Figures 4e and 4f displaying that velocities for the low flow are drastically lower than in high flows. The quantitative estimates for the dune heights are obtained with BTT applied for the longitudinal segments visualized in Figures 2b and 2c. Using the BTT method, representative height and wavelengths were determined to be 1.73-m high and 98-m long for the low-flow case and 3.22-m high and 82.7-m long for the high flow. These results are in contrast with the theoretical findings of M. S. Yalin (1964) and Van Rijn (1984) for dunes in equilibrium whereby it is found that dune wavelength is mainly controlled by the water depth. However, these trends are confirmed by the analysis with an alternative method conducted by Ramirez et al. (2018) for the same flows that is, the heights and wavelengths for the same locations were 1.44 and 80.1 m for the low flow and 3.1 and 64.5 m for the high flow, respectively. As expected, the differences between the bed geometries for the two flows result in commensurate differences between the transported sediment (see Figures 4g and 4h). A comprehensive discussion of these discrepancies would be useful both for setting the capabilities of the AMV in the proper context and/or explaining what assumptions or mechanisms in the models might produce these discrepancies. The essential aspect for this paper context is that AMV offers new perspectives on the bedload transport processes that could not be quantified before.

4. AMV Evaluation Against Other Methods for Estimation of the Bedload Transport Rates

4.1. Comparisons Across Indirect Estimation Methods Based on Dune-Tracking Approaches

The across-method comparison presented here involves four approaches developed independently by a research team at IIHR, a team at Budapest University of Technology and Economics (BME), and two other teams at US Army Corps of Engineers (USACE). The comparison is using identical input as provided by the MBES raw

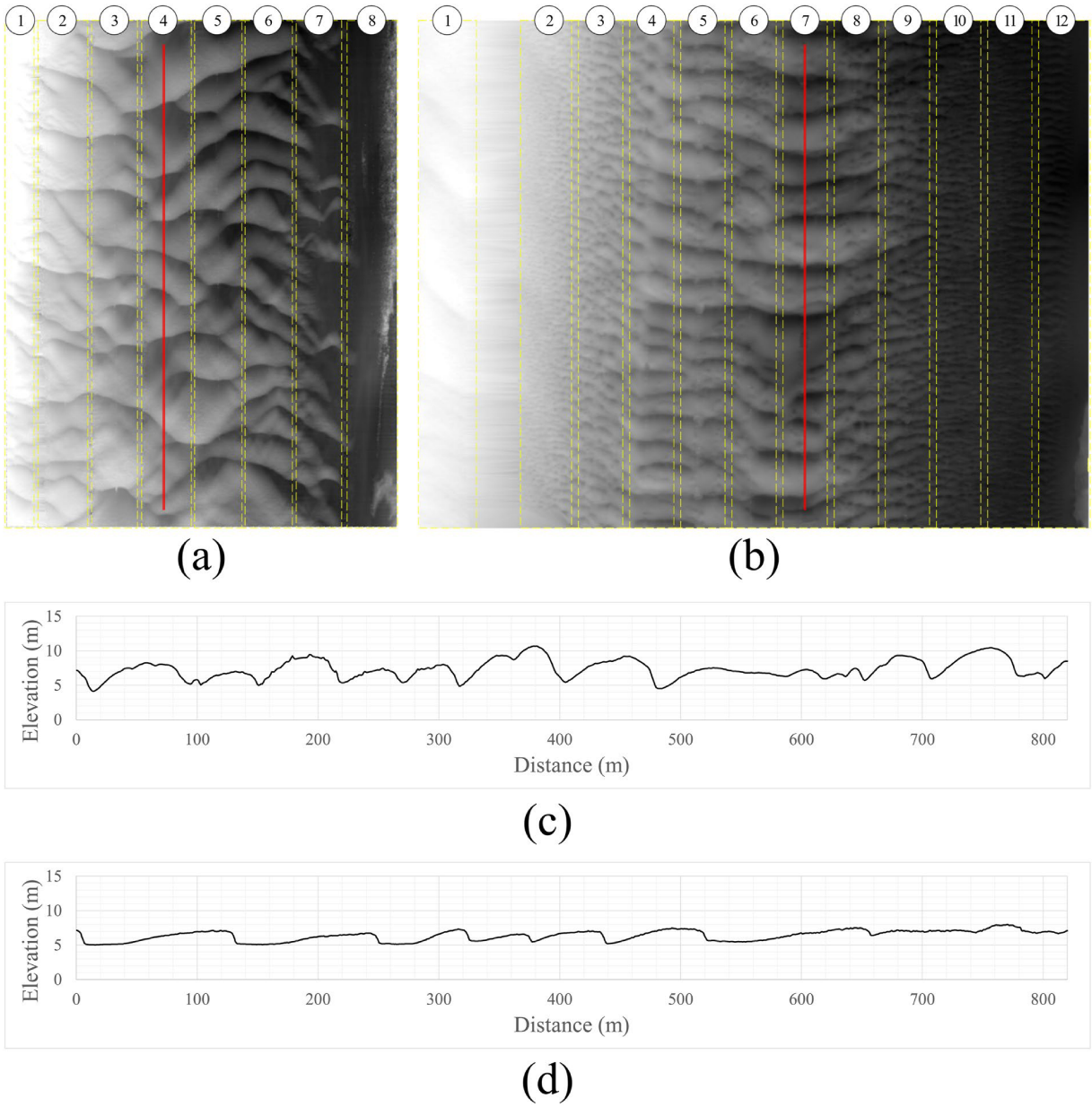

Figure 3. Illustration of the bedforms at low- and high-flow conditions: (a) mapped area at low flow, (b) mapped area at high flows, (c) longitudinal profile at low flow; (d) longitudinal profile at high flow.

data acquired in the high flow case for the Mississippi River described above. The four methods use different algorithms to estimate the same parameters, hence they are inherently associated with a degree of subjectivity because they involve selection of procedures and thresholds for the estimated parameters. These selections are based on engineering judgment continuously optimized through repeated algorithms' implementations in various measurement conditions. The comparison entails bedload rate estimation, the most-commonly goal of the AMV measurements, as well as components of the estimation methods used in the data acquisition and processing (i.e., estimated average bedform heights and wavelengths). Given that the estimation of the parameters and final results are determined with different processing algorithms, there is an expectation that the compared outputs display differences, and those differences offer opportunities for critical discussions and additional inferences.

For four different methods discussed herein are labeled as: AMV-IIHR (as described in Section 3), AMV-BME, ISSDOTv2, and USACE-bedform (USACE-B). The first three methods are used to estimate bedload transport

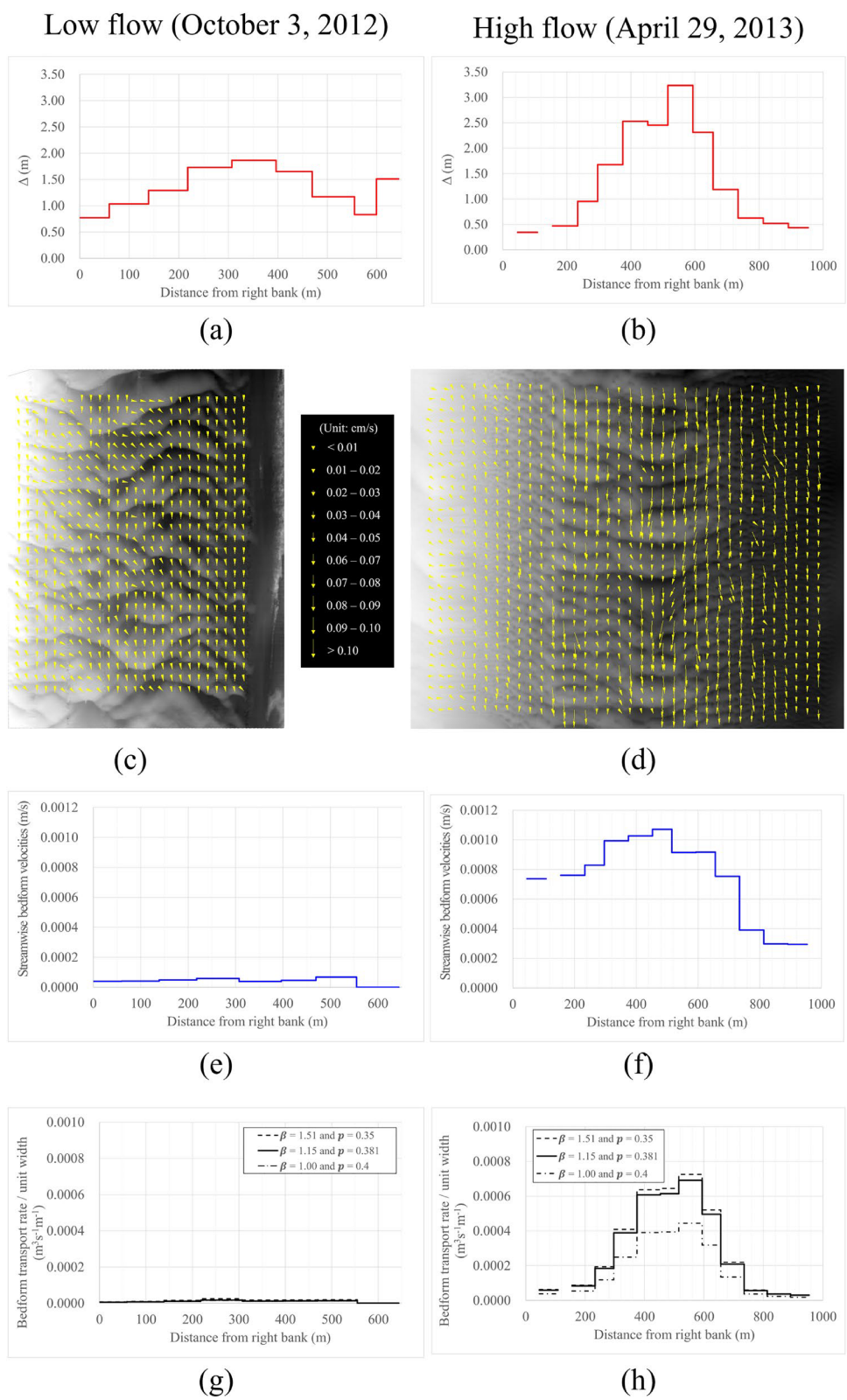

Figure 4. Results of the acoustic mapping velocimetry implementation on the multi-beam echo-sounders repeated maps acquired at low flow (3 October 2012) and high flow (29 April 2013); (a) and (b) cross-sectional distribution of the bedform wavelengths; (c) and (d) whole-field velocity distribution obtained with HGPIV; (e) and (f) cross-sectional distribution of the bedform velocities; (g) and (h) cross-sectional distributions of the bedform mass transport rates.

Table 3
Comparison of Components of Bedload Transport Rates Obtained With Various Methods Applied to the Multi-Beam Echo-Sounders Bathymetric Survey Acquired in High-Flow Conditions in the Mississippi River (29 April 2013) Along the Longitudinal Bedform Profile Shown in Figure 2c

	Bedform morpho-dynamic characteristics							
	Wavelength, Δ, (m)		Height, λ, (m)		Migration velocity, v_b, (ms^{-1})		Bedload transport rate, q_b, ($kgs^{-1}m^{-1}$)	
Method	Absolute	Difference (%)	Absolute	Difference (%)	Absolute	Difference (%)	Absolute	Difference (%)
AMV-IIHR[a]	82.7	–	3.22	–	0.0009	–	2.361	–
AMV-BME	79.1	−4	2.81	−13	0.0007	−22	1.923	−19
ISSDOTv2	n/a	–	n/a	–	n/a	–	1.87	−20
USACE-B	64.5	−22	3.1	−4				

[a]Reference for the comparison.

rates, while the last one only estimates geometrical characteristics of the bedforms. The first two methods are based on IV applied to acoustic maps while the third approach is based on scour-deposition differential analysis applied to longitudinal bedform profiles. The first two methods derive geometrical characteristics of a representative bedform using the BTT method developed by Van der Mack et al. (2008) applied to the wave train enclosed in a swath (Baranya et al., 2022; You, Muste, et al., 2021). The ISSDOTv2 method uses an in-house developed approach whereby the transport rates for each individual wave are determined and weighted to determine the averaged bedload transport rate at various locations across the channel (McAlpin et al., 2022). The USACE-B method estimates representative bedform characteristics by defining the dunes via the zero-crossing approach applied to a detrended longitudinal bathymetric profile (Ramirez et al., 2018). Results obtained with the four aforementioned methods are compared in Table 3 (along the longitudinal profiles indicated with red line in Figure 2c) and Figure 5 (across the river cross-section within the MBES surveyed reach).

Table 3 compares the average geometrical bedform characteristics and the rates of bedload transport as determined with AMV-IIHR, AMV-BME, ISSDOTv2, and USACE-B methods (as appropriate) using identical acoustic maps as raw data. The dune wavelength is not used in the calculation of the bedload rate with the Exner equation, but it is an important variable for characterization of the bedform migration and is perhaps the most accurately determined parameter from the high-density MBES surveys. The bedform wavelength is an important parameter for the design of any dune-tracking based method as the number of surveyed dunes is perhaps the largest contributor to the reliability of the measurements with this method (You, Muste, et al., 2021). The longitudinal bedform profile (indicated with red line in Figure 2c) is representative for the comparison illustrated herein as it is located in the area with the largest dunes, hence contributing substantially to the total bedload transport rates (see also the peak of the bedload transport rate shown in Figure 5). While this analysis can be repeated for multiple longitudinal profiles, we limit our comparison to just one given that the purpose of this

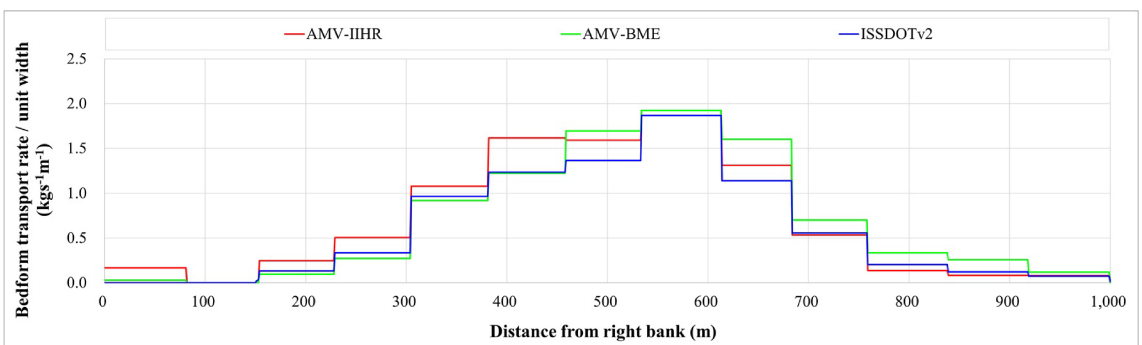

Figure 5. Comparison of the bedload transport rate cross-sectional distributions estimated by AMV-IIHR, AMV-BME and ISSDOTv2 for the high flow conditions on 29 April 2013.

paper is to substantiate differences in the estimation methods with the goal to infer insights on their capabilities and limitations. Table 3 also contains the migration velocity along the same representative line determined by AMV-IIHR and AMV-MBE, the only methods (out of the four presented here) that determine this variable. The addition of this variable is made here for completeness as it is an indirect by-product of the AMV-based measurements. Collectively, the set of three bedform parameters, that is, wavelength, height, and migration velocity provide a robust description of the bedform morpho-hydrodynamics. Finally, Table 3 contains the estimate of the bedload transport rates estimated by AMV-IIHR, AMV-BME, and ISSDOTv2. Figure 5 displays the average bedload transport rates estimated per individual swath acquired across the river width as estimated with the three above-mentioned methods.

The agreement between the estimated methods along the representative line shown in Figure 2c using the four methods is not particularly good indicating the impact of difference in the approaches for determining bed geometry and dynamics. The differences between AMV-IIHR and AMV-BME are highlighting that even when using quite similar approaches the difference in selecting the processing parameters can sensibly affect the results. The latter aspect is substantiated by the 13% difference in the estimation of bedform height and 22% in the migration velocity estimated with AMV-IIHR and AMV-BME despite that these bedform transport rates approaches are the most similar among the four analyzed here. While AMV-BME and ISSDOTv2 estimates are considerably closer compared with AMV-IIHR, it can be noticed that the results obtained with the three methods display the largest differences in the area of the largest size dunes. The difference between AMV-IIHR and AMV-BME migration velocity is potentially associated with the use of different IV algorithms (i.e., OF combined with cross-correlation, and stand-alone cross-correlation, respectively) and the different IV parameters used for the IV (i.e., interrogation area sizes of 128 × 128 m and of 40 × 40 m for AMV-IIHR and AMV-BME, respectively). The difference between AMV-IIHR and AMV-BME bedform height is associated with the different selection of the BTT internal processing parameters. The difference in the bedload transport rate is compounding the effect of the two uncertainty sources.

The AMV-based protocols use dune dynamics for dune tracking, while ISSDOTv2 is based on bedform geometry differences. The fourth method is solely based on the statistical analysis of the zero-line bedform reference. Notably, AMV-IIHR and AMV-BME can track two-dimensional transport (i.e., the streamwise and lateral components of the bedform movement) in contrast with ISSDOTv2 which is a one-directional estimation method. For the present case, the estimation of the bedload rates with AMV was done by excluding the lateral component of the movement. The accuracy of the results obtained with techniques such as ISSDOTv2 can be influenced by the positioning and direction of the profile in the river, that in turn overestimates dune length and volumes and underestimate bedload transport rates (Wilbers, 2004). A more rigorous analysis of the above-illustrated differences might reveal what is generating systematic differences and how to avoid them. However, definitive conclusions on which method is more accurate cannot be drawn in the absence of a reliable method for ground-truthing.

4.2. Comparison With Direct Morphologic Estimation Methods Based on Semi-Empirical Approaches

The ground-truthing of the measurement output is critical for any newly developed measurement technique. This is especially important in this river morphology area where there are no widely accepted references and, as a consequence, the reliability of data produced by various instruments and predictors is highly scrutinized. A realistic validation of the AMV would ideally entails direct measurements with alternative instruments or procedures. Notably this would include comparisons with physical sampling at fixed points (Gray et al., 2010) or ADCP bottom-tracking (Gasparato et al., 2022). Such comparisons are attempted for the high-flow case in the recent paper by Baranya et al. (2022). With the intent to support AMV implementation at new sites, in this section we compare the data outputted by the AMV-IIHR workflow against conventional analytical methods used to predict bedload transport rates using direct morphologic methods (i.e., formula stemming from semi-empirical or purely analytic relationships).

There is a plethora of analytical and semi-empirical frameworks for the estimation of bedload transport rates in steady flows with sediment transport in equilibrium regime (e.g., Armijos et al., 2021; ASCE, 2008). However, in the present context preference in selecting the bedload transport rate formula is given to the reliance of the predictors on a small number of variables and their easiness to determine in situ. Some of these measurements can be estimated without conducting new measurements by inspecting previous records that, most probably, contain variables such as river depth, bulk velocity, and discharge acquired at the site or in its vicinity. More complex

Table 4
Comparison of AMV-IIHR Estimates With Various Predictors for Dune Geometry and Dynamics (the High-Flow Case, 29 April 2013) Along the Longitudinal Bedform Profile Shown in Figure 2c

	Bedform morpho-dynamics characteristics						Bedload transport rate q_b, ($kgs^{-1}m^{-1}$)	
	Wavelength Δ, (m)		Height λ, (m)		Migration velocity v_b, (ms^{-1})			
Method	Absolute	%	Absolute	%	Absolute	%	Absolute	%
AMV-IIHR	82.7	–	3.22	–	0.0009		2361	
Group A								
ASCE (2008)	41.0	−50	3.17	−2				
Bradley and Venditti (2017)	53.8	−35	3.06	−5				
Cisneros et al. (2020)	105.7	+28	1.9	−41				
Van Rijn (1984)	116.8	+41	0.07	−98				
Allen (1968)	85.3	+3	2.3	−29				
Group B								
Dillo (1960)					0.0005	+44		
Group C								
Van Rijn (1984)							0.49	−79
Engelund and Hansen (1967)							3.16	+34

relationships based on difficult to obtain measurements (such as critical flow velocity, shear stress, terminal fall velocity) are avoided here as the predictors are used to design field experiments rather than validate results regarding bedform development from experimental and analytical investigations. Similarly with the previous comparison, the discussion in this section uses the AMV-IIHR results as the reference for the comparison. We structure this comparison around three groups of variables as shown below:

- Group A: geometry of the bedforms
- Group B: bedform migration velocities
- Group C: bedload transport rates

The most important group for practical purposes is Group C. However, the other two groups are highly relevant for the transport process understanding and for designing the AMV in-situ experiments at new measurement sites.

Wilbers (2004) tested with field data the validity of several analytical and semi-empirical predictors for dune height and dune length (Group A) in steady and uniform flows and concluded that only five predictors are reliable. Based on these findings we select the best two of them for testing against our measurements, that is, Allen (1968) and Van Rijn (1984). Wilbers (2004) also offers compilations of data and relationships that link dune wavelength and dune height for various steady-flow conditions. The predictors for the bedform migration velocity (Group B) are scarce, for the most part because of the difficulty taking this type of measurement (Tabesh et al., 2022; Wilbers, 2004). In this respect, techniques such as AMV can play a critical role as the migration velocity can be determined quite easily from processing repeated acoustic maps with visible bedform crests. The availability of predictors for bedform velocity is essentials for the implementation of the AMV as the bedform migration rates prescribe the optimal time between repeated survey maps as required by the IV rules of thumb (Adrian, 1991). Most of the predictors for bedload transport rates (Group C) are based on governing relationships between flow strength, water depth, and bed material grainsize. Recent studies that compared observed and predicted characteristics of the bedload transport rates determined the Engelund and Hansen (1967) and Van Rijn (1984) relationships show the best agreement with field measurements in natural sand-bed rivers (Armijos et al., 2021; Kleinhans, 2002). Table 4 displays variable estimates using several formulas pertaining to each group. The detailed calculations for all the used formula are provided in the Supplemental Material.

The results provided by the predicting relationships in Table 4 are quite different from the AMV-IIHR measurements used herein as reference. There is no indication of a persistent bias in the estimation of the bedform characteristics or of the bedload transport rates acquired with AMV. This disagreement is not surprising as quantifying bedform geometrical and dynamic characteristics is known to be notoriously difficult (Ancey, 2020).

Actually (Duffy, 2006), concludes that the predictors' outcomes can vary over several order of magnitudes even if the input parameters are identical. Moreover, using predictors based on the same physical principles may display uncertainties in the results that can vary by an order of magnitude (Patalano et al., 2022; Tsubaki et al., 2018).

5. Discussions

The above-presented results show the capability of AMV for characterizing critical features of the bedform migration relevant for science and practice using MBES data acquired in a large river. While the estimation of bedform characteristics and estimation of bedload transport rates might be the most useful practical results, the AMV provides information on dune steepness and mean stoss- and lee-side angles. We also note that the instruments used for data acquisition as well as the measurement protocols associated with AMV are increasingly mature and widespread. The image processing component of the AMV is analog to the Large-Scale Particle Image Velocimetry (LSPIV) technique where the PIV concepts are applied to image patterns rather than images of a group of particles (Muste et al., 2008). Patterns are defined as continuous shapes created by gray-level pixel intensity distributions. Consequently, each pixel in the interrogated area contribute to the cross-correlation, not only the pixels defining the individual particles. Both methods assume the patterns remain “rigid non-deformable” between image pairs.

Recent papers by Baranya et al. (2022) and You, Muste, et al. (2021) demonstrate the impact of data acquisition protocols on the AMV image processing component. We note here that the judicious selection of the size of the Interrogation Areas and the time step between image pairs is critical for the accuracy of the bedform dynamics estimates. Similarly to LSPIV, this selection is based on a trial-and-error process that requires experience with the technique and understanding of the bedform regime and dynamics. As a consequence, there is a dosage of subjectivity in the estimations that is closely related to the users' skills. However, the selection process is quite intuitive (as it is based on visual observation) and reliable, as proven by multiple comparisons whereby the LSPIV-estimated velocity distributions over the cross section and the discharge estimates are in good agreement with alternative measurements with well-established discharge estimation (Muste et al., 2011).

The AMV results presented herein cover a range of bedform scales at one site (from ripples to primary and secondary dunes) enabling identification of bedform migration directions (1D, 2D or 3D), as illustrated in Figure 6a. With proper acoustic map resolution and careful selection of the processing parameters, the AMV can detect both dune migration as a whole as well as the movement of secondary dunes or ripples within the dune wavelength, as shown in Figure 6b. Note that the vectors associated with the bedforms in this figure indicate that the ripples move faster than the dune crest (as shown by the larger magnitude vectors estimate between those corresponding to the dune crest). However, because the size of the interrogation area selected for the image processing in this paper is close to the size of the largest dunes the resultant velocity estimates are mostly valid for the representative dune within the wave train (see Table 3). With further adjustments of the processing parameters, the AMV can reveal more details of one or the other bed migration transport form. This latter AMV capability is important as it enables to distinguish between primary and secondary migration of bedforms.

Despite the above-highlighted AMV capabilities, the relatively large differences in the estimation of sub-components and final results obtained with the two AMV versions, that is, AMV-IIHR and AMV-BME, indicate that the AMV has not yet passed the evaluation stage and need to be further optimized for becoming a reliable in situ measurement approach for comprehensive characterization of the bedload processes. Given that this and our prior AMV in-situ studies entail data from the same case study (i.e., MBES data repeatedly acquired over a cross section of the Mississippi River), the outcomes of these discussions can be considered indicative rather than definitive. However, this analysis represents a good precursor for a full-fledged AMV uncertainty analysis. Along this line, a good starting point is the list of individual sources of uncertainty listed in Table 2 (last column) that can be further tested over their range of possible occurrence. Furthermore, it seems that quantifying both types of bedforms with the same image processing parameters, as it is done in this paper, might lead to errors in the bedload transport rate estimates as noted by Baranya et al. (2022). It seems that the best implementation strategy for estimation of the bedform dynamics with AMV is to adopt a scale-dependent characterization as suggested by Guala et al. (2014). This strategy might call for multiple image processing runs; one run applied to areas encompassing several large dunes (as done in this paper) and a separate run for areas contained within a single wavelength.

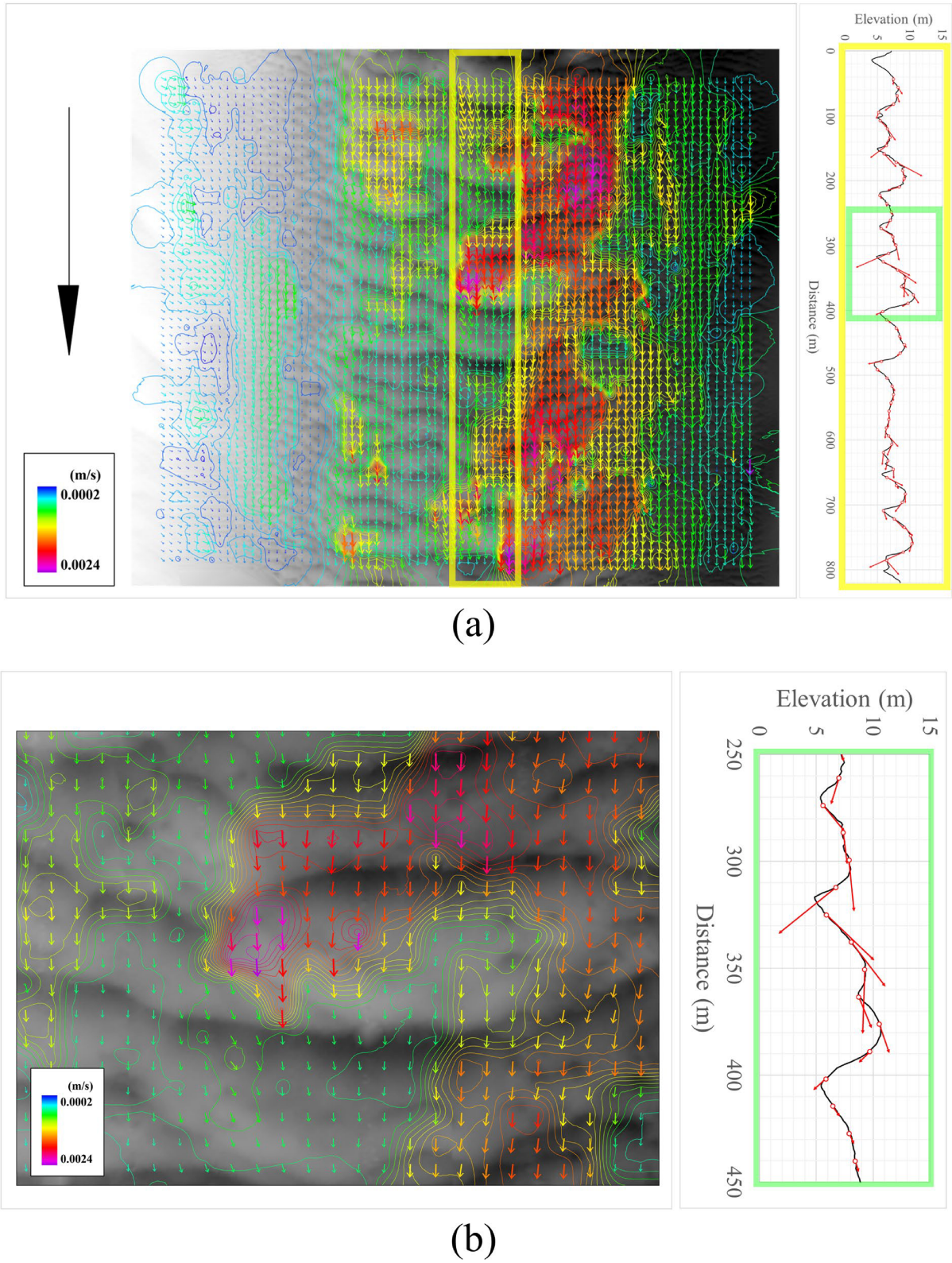

Figure 6. Whole-field velocities produced by acoustic mapping velocimetry; (a) over the entire acoustic map; (b) over an area commensurate with the size of a bedform.

The AMV usage is still in early developmental stages and requires further refinements of its implementation protocols. One of the major hurdles for AMV implementation is the selection of the proper data acquisition protocols and processing parameters for measurements at new locations. This selection is based on anticipating the actual type of morpho-dynamic processes at the time and location of the measurements and their impact on the results. The anticipation of local sediment transport processes cannot be attained without full understanding of the bedform migration mechanics and of the investigative frameworks used to describe them. Much improvement is expected in this area as the diversity of analytical and semi-empirical approaches and formulations are inconsistent among themselves, as demonstrated by the results presented in Table 4. The results presented in this paper indicate that emerging approaches such as AMV in conjunction with high-resolution bathymetric data can shed light on the validity of these formulations.

In the absence of analytical support, there is a need for a careful inspection of the longitudinal bedform profiles using prior measurements (even if they are sporadic) or diagnostic measurements prior to AMV implementation. This need stems from the fact that there are several aspects of bedload transport that will change the outcomes of the AMV, as well as other DTM-based results, even if the measurement technique adequately follows rules of thumb applied to the processing components. Even for this simplest form of bedform movement (i.e., the steady flow with sediment transport in equilibrium), there are subtleties that must be considered in producing reliable measurements with AMV. For this purpose, we first caution on some salient aspects of steady flows with sediment transport in equilibrium. This sediment transport regime is well documented by analytical and semi-empirical formulations that enables the design of the experiments and setting of the AMV processing parameters (e.g., Van Rijn, 1984; S. Yalin, 1964). Subsequently, some frugal considerations on unsteady flows are reported.

5.1. Steady Flows Regime With Dune Superposition

Most of the reported field measurements characterize steady flows based on quasi-constant flow discharge or stage during the measurements. In this scenario, one possible alternative is that all the sediment transported by erosion from the stoss side of the bedform is subsequently deposited on its lee side. There are steady transport situations, where secondary dunes are superimposed upon the spatially varying primary dunes. Superimposed dunes can affect the conversion of the dune migration rate into a bedload transport rate. The consequences of not accounting for the impact of secondary dunes on the total bedload transport are extensively discussed in Wilbers (2004). These types of flows are often encountered at higher flow stages (Huntley et al., 1991). For this reason, if knowledge of typical maximum local flow stage is not available, then the measured bedload transport rates must be considered to be a lower estimator of bedload transport (Knaapen et al., 2005). Fortunately, the visual nature of the AMV-derived maps acquired with MBES provide a detailed picture of the riverbed section of interest that facilitate the recognition of these peculiar bedform aspects. The data provided by AMV enables investigation of the 3-D dune shapes and their development and if preferential transport pathways are developed within the stream reach.

5.2. Unsteady Flows

This type of flows occurs during flood wave propagation in inland rivers and are ubiquitous in rivers located in coastal areas. The distinct temporal variations on the rising and falling limbs of the flow hydrograph require adaptation of the AMV data acquisition and processing parameters. The implementation of AMV for capturing bedform migration for these types of flow is a complex endeavor. There are much less analytical and semi-empirical formulations for predicting bedform migration in unsteady flows and only scarce measurements documenting these flows. Direct measurements conducted by Lisimenka et al. (2022) illustrate that the dune height and length are larger during the falling limb than the rising limb for the same streamflow. Wilbers and Ten Brinke (2003) found that the relatively fast changes in hydraulic conditions during flood wave propagation favor the formation of superimposed bedforms. Wilbers (2004) showed that the dune growth and decay and migration rate are widely different during floods, and these differences are related to differences in grain size of the bed and to differences in the distribution of discharge over the main channel and the floodplain. It is obvious unsteady sediment transport needs more experimental evidence to properly inform the AMV implementation.

6. Conclusions

The presentation of the AMV capabilities to explore bedform dynamics over a range of spatio-temporal scales demonstrates that the technique is effective in providing comprehensive information on bedform morphometric

parameters and migration rates. The paper assembles the factors that influence the reliability of the AMV in field situations and recommends complementary guidelines to those presented in the paper by Baranya et al. (2022) and You, Muste, et al. (2021). The presented measurements demonstrate that AMV reveals fine details of the bedform migration dynamics that are not readily-available from measurements with other methods. The present evaluation is much needed as, similarly to other non-intrusive measurement methods, AMV uses remote-sensed aspects of the process targeted by the measurements relying extensively on multiple assumptions and parameters that are site-specific. These assumptions and parameters are associated with all aspects of the AMV implementation, from the acquisition of the repeated bathymetric maps to the estimation of bedload transport rates. Finally, we contend that AMV is becoming a reasonable option for determining bedform characteristics and bedload transport rates which are extremely important to addressing basic questions about bedform mechanics developing over a broad range of spatio-temporal scales. However, full validation of AMV cannot be accomplished without a proven convergence of alternative in-situ measurements and analytical considerations that account for the wide range of factors that influence the bedform dynamics at a specific site.

Conflict of Interest

The authors declare no conflicts of interest relevant to this study.

Data Availability Statement

The data set is available in You (2023). The software illustrated in Figures 3a, 3b, 4e, 4f, and 6 have been previously developed and used, cited in this paper (You, Kim, et al., 2021).

Acknowledgments
The authors appreciate the input provided by the anonymous reviewers that substantially improved the paper content. We also acknowledge the funding provided by the US Geological Survey Cooperative Grant Agreement #Gl9AC00257. The first author was partially supported by the NSF award EAR 1948944. This work was supported by Korea Environment Industry & Technology Institute (KEITI) through Advanced Water Management Research Program, funded by Korea Ministry of Environment (MOE) (1615012820). Finally, the authors acknowledge the assistance provided by Kyeongdong Kim with Dankook University in submitting the final manuscript.

References

Aberle, J., Coleman, S. E., & Nikora, V. I. (2012). Bed load transport by bed form migration. *Acta Geophysica*, *60*(6), 1720–1743. https://doi.org/10.2478/s11600-012-0076-y

Abraham, D., & Kuhnle, R. (2006). Using high resolution bathymetric data for measuring bed-load transport. In *Proc., 8th federal interagency sedimentation conference and 3rd federal interagency hydrologic modeling conference* (pp. 619–626). US Subcommittee on Sediment.

Abraham, D., Kuhnle, R. A., & Odgaard, A. J. (2011). Validation of bed-load transport measurements with time-sequenced bathymetric data. *Journal of Hydraulic Engineering*, *137*(7), 723–728. https://doi.org/10.1061/(ASCE)HY.1943-7900.0000357

Adrian, R. J. (1991). Particle-imaging techniques for experimental fluid mechanics. *Annual Review of Fluid Mechanics*, *23*(1), 261–304. https://doi.org/10.1146/annurev.fl.23.010191.001401

Allen, J. R. L. (1968). The nature and origin of bed-form hierarchies. *Sedimentology*, *10*(3), 161–182. https://doi.org/10.1111/j.1365-3091.1968.tb01110.x

Ancey, C. (2020). Bedload transport: A walk between randomness and determinism. Part 1. The state of the art. *Journal of Hydraulic Research*, *58*(1), 1–17. https://doi.org/10.1080/00221686.2019.1702594

Armijos, E., Merten, G. H., Groten, J. T., Ellison, C. A., & Lisiecki, L. U. (2021). Performance of bedload sediment transport formulas applied to the Lower Minnesota River. *Journal of Hydrologic Engineering*, *26*(7), 05021014. https://doi.org/10.1061/(ASCE)HE.1943-5584.0002107

ASCE. (2008). In M. Garcia (Ed.), *Sedimentation engineering: Processes, management, modeling, and practice*. American Society of Civil Engineers.

Ashmore, P. E., & Church, M. (1998). Sediment transport and river morphology: A paradigm for study. *Gravel-Bed Rivers in the Environment*, *345*, 115–139.

Baranya, S., Fleit, G., Tsubaki, R., Muste, M., & Józsa, J. (2022). Bedload estimation in large sand-bed rivers using Acoustic Mapping Velocimetry (AMV). *Geomorphology*, *424*, 14. 108562. https://doi.org/10.1016/j.geomorph.2022.108562

Baranya, S., Muste, M., Abraham, D., & Pratt, T. C. (2016). Acoustic mapping velocimetry for in-situ bedload transport estimation. In *River flow conference*.

Best, J. (2005). The fluid dynamics of river dunes: A review and some future research directions. *Journal of Geophysical Research: Earth Surface*, *110*(F4), F04S02. https://doi.org/10.1029/2004JF000218

Bradley, R. W., & Venditti, J. G. (2017). Reevaluating dune scaling relations. *Earth-Science Reviews*, *165*, 356–376. https://doi.org/10.1016/j.earscirev.2016.11.004

Cisneros, J., Best, J., van Dijk, T., Pas de Almeida, R., Amsler, M., Boldt, J., et al. (2020). Dunes in the world's big rivers are characterized by low-angle lee-side slopes and a complex shape. *Nature Geoscience*, *13*(2), 156–162. https://doi.org/10.1038/s41561-019-0511-7

Claude, N., Rodrigues, S., Bustillo, V., Bréhéret, J. G., Macaire, J. J., & Jugé, P. (2012). Estimating bedload transport in a large sand–gravel bed river from direct sampling, dune tracking and empirical formulas. *Geomorphology*, *179*, 40–57. https://doi.org/10.1016/j.geomorph.2012.07.030

Conevski, S., Guerrero, M., Winterscheid, A., Rennie, C. D., & Ruther, N. (2020). Acoustic sampling effects on bedload quantification using acoustic Doppler current profilers. *Journal of Hydraulic Research*, *58*(6), 982–1000. https://doi.org/10.1080/00221686.2019.1703047

Detert, M. (2021). How to avoid and correct biased riverine surface image velocimetry. *Water Resources Research*, *57*(2), e2020WR027833. https://doi.org/10.1029/2020WR027833

Dillo, H. (1960). *Sandwanderung in Tideflüssen: Technische Hochschule*. Franzius-Institut für Grund-und Wasserbau.

Dinehart, R. L. (2002). Bedform movement recorded by sequential single-beam surveys in tidal rivers. *Journal of Hydrology*, *258*(1–4), 25–39. https://doi.org/10.1016/S0022-1694(01)00558-3

Duffy, G. P. (2006). *Bedform migration and associated sand transport on a banner bank: Application of repetitive multibeam surveying and tidal current measurement to the estimation of sediment transport*. The Univ. of New Brunswick.

Engelund, F., & Hansen, E. (1967). *A monograph on sediment transport in alluvial streams*. Teknisk Vorlag.
Ergenzinger, P., & De Jong, C. (2003). *Perspectives on bed load measurement* (pp. 113–125). IAHS Publication.
Exner, F. M. (1931). Zur dynamik der bewegungsformen auf der erdoberfläche. *Ergebnisse der kosmischen Physik*, *1*, 373–445. https://doi.org/10.4157/grj.8.341
Gasparato, D., Herrera Gomez, L. V., Ravazzani, G., & Mancini, M. (2022). Potentiality of bedload measures using Acoustic Doppler Current profiler technique. In *EGU general assembly conference abstracts (No. EGU22-5978)*. https://doi.org/10.5194/egusphere-egu22-5978
Gibb, J. P., Barcelona, M. J., Ritchey, J. D., & LeFaivre, M. H. (1984). *Effective porosity of geologic materials: First annual report*. Illinois State Water Survey.
Gomez, B. (1991). Bedload transport. *Earth-Science Reviews*, *31*(2), 89–132. https://doi.org/10.1016/0012-8252(91)90017-A
Gray, J. R., Laronne, J. B., & Marr, J. D. (2010). *Bedload-surrogate monitoring technologies* (p. 37). US Department of the Interior, US Geological Survey.
Guala, M., Singh, A., BadHeartBull, N., & Foufoula-Georgiou, E. (2014). Spectral description of migrating bed forms and sediment transport. *Journal Geophysical Research: Earth Surface*, *119*(2), 123–137. https://doi.org/10.1002/2013JF002759
Gutierrez, R. R., Mallma, J. A., Núñez-González, F., Link, O., & Abad, J. D. (2018). Bedforms-ATM, an open source software to analyze the scale-based hierarchies and dimensionality of natural bed forms. *SoftwareX*, *7*, 184–189. https://doi.org/10.1016/j.softx.2018.06.001
Holmes, R. R., Jr. (2010). *Measurement of bedload transport in sand-bed rivers: A look at two indirect sampling methods*. US Geological Survey.
Huntley, D. A., Amos, C. L., Williams, J. J., & Humphery, J. D. (1991). Estimating bedload transport on continental shelves by observations of ripple migration: An assessment. In *EUROMECH colloquium on sand transport in rivers, estuaries and the sea* (Vol. 262, pp. 17–24).
Jones, K. E., Abraham, D. D., & McAlpin, T. O. (2018). *Bed-load and water surface measurements during the 2011 Mississippi River Flood at Vicksburg, Mississippi* (MRG&P Report No. 18). US Army Engineer Research and Development Center.
Kemp, K. K. (1993). Environmental modeling with GIS: A strategy for dealing with spatial continuity (Doctoral dissertation). University of California.
Kleinhans, M. G. (2002). Sorting out sand and gravel: Sediment transport and deposition in sand-gravel bed rivers (Doctoral dissertation). Utrecht University.
Knaapen, M. A. F. (2004). Measuring sand wave migration in the field. Comparison of different data sources and an error analysis. In *Marine sandwave dynamics and river dune dynamics II, international workshop* (pp. 152–159). University of Twente.
Knaapen, M. A. F., van Bergen Henegouw, C. N., & Hu, Y. Y. (2005). Quantifying bedform migration using multi-beam sonar. *Geo-Marine Letters*, *25*(5), 306–314. https://doi.org/10.1007/s00367-005-0005-z
Leary, K. C., & Buscombe, D. (2020). Estimating sand bed load in rivers by tracking dunes: A comparison of methods based on bed elevation time series. *Earth Surface Dynamics*, *8*(1), 161–172. https://doi.org/10.5194/esurf-8-161-2020
Le Guern, J., Rodrigues, S., Geay, T., Zanker, S., Hauet, A., Tassi, P., et al. (2021). Relevance of acoustic methods to quantify bedload transport and bedform dynamics in a large sandy-gravel-bed river. *Earth Surface Dynamics*, *9*(3), 423–444. https://doi.org/10.5194/esurf-9-423-2021
Lisimenka, A., Kubicki, A., & Kałas, M. (2022). Bedforms evolution in the Vistula River mouth during extreme flood event, southern Baltic Sea. *Oceanologia*, *64*(1), 212–226. https://doi.org/10.1016/j.oceano.2021.10.005
Marquis, G. A., & Roy, A. G. (2012). Using multiple bed load measurements: Toward the identification of bed dilation and contraction in gravel-bed rivers. *Journal of Geophysical Research: Earth Surface*, *117*(F1), F01014. https://doi.org/10.1029/2011JF002120
McAlpin, T. O., Wren, D. G., Jones, K. E., Abraham, D. D., & Kuhnle, R. A. (2022). Bed-load validation for ISSDOTv2. *Journal of Hydraulic Engineering*, *148*(3), 04022001. https://doi.org/10.1061/(ASCE)HY.1943-7900.0001968
Muste, M., Abraham, D., Jones, K., Wagner, D., & Whaling, A. (2019). *In-situ bedload measurements using multi-beam echosounders and acoustic current Doppler profilers*. US Geological Survey Cooperative Agreement# G19AC00257. USGS National Grants Branch.
Muste, M., Baranya, S., Tsubaki, R., Kim, D., Ho, H., Tsai, H., & Law, D. (2016). Acoustic mapping velocimetry. *Water Resources Research*, *52*(5), 4132–4150. https://doi.org/10.1002/2015WR018354
Muste, M., Fujita, I., & Hauet, A. (2008). Large-scale particle image velocimetry for measurements in riverine environments. *Water Resources Research*, *46*(4), W00D19. https://doi.org/10.1029/2008WR006950
Muste, M., Kim, D., & Ho, H.-C. (2011). "Considerations on direct stream flow measurements using video imagery: Outlook and research needs," Special Issue - Field and laboratory particle image velocimetry and its application in hydraulics research and flow measurements. *Journal of Hydro-environment Research*, *5*(4), 289–300. https://doi.org/10.1016/j.jher.2010.11.002
Nittrouer, J. A., Allison, M. A., & Campanella, R. (2008). Bedform transport rates for the lowermost Mississippi River. *Journal of Geophysical Research*, *113*(F3), F03004. https://doi.org/10.1029/2007JF000795
Patalano, A., Ligorria, A. I. H., Lozada, J. M. D., & García, C. M. (2022). Image-based migration velocity and dune length in clear water rivers. *Flow Measurement and Instrumentation*, *86*, 102174. https://doi.org/10.1016/j.flowmeasinst.2022.102174
Raffel, M., Willert, C. E., & Kompenhans, J. (2007). *Particle image velocimetry - a practical guide* (2nd ed.). Springer Verlag.
Ramirez, M. T., Smith, S. J., Lewis, J. W., & Pratt, T. C. (2018). *Mississippi river bedform roughness and streamflow conditions near Vicksburg, Mississippi: Data collection summary and analysis* (MRG&P Report No. 22). US Army Engineer Research and Development Center.
Reid, I., Layman, J. T., & Frostick, L. E. (1980). The continuous measurement of bedload discharge. *Journal of Hydraulic Research*, *18*(3), 243–249. https://doi.org/10.1080/00221688009499550
Rennie, C. D., & Millar, R. G. (2004). Measurement of the spatial distribution of fluvial bedload transport velocity in both sand and gravel. *Earth Surface Processes and Landforms: The Journal of the British Geomorphological Research Group*, *29*(10), 1173–1193. https://doi.org/10.1002/esp.1074
Simons, D. B., Richardson, E. V., & Nordin, C. F. (1965). *Bedload equation for ripples and dunes*. Professional paper 462-H. US Government Printing Office. https://doi.org/10.3133/pp462H
Tabesh, M., Reich, J., & Winterscheid, A. (2022). Temporal resolution of echosounding measurements for assessing bedload transport rates via dune tracking. In *EGU general assembly conference abstracts (No. EGU22-6369)*. https://doi.org/10.5194/egusphere-egu22-6369
Thorne, P. D. (2014). An overview of underwater sound generated by interparticle collisions and its application to the measurements of coarse sediment bedload transport. *Earth Surface Dynamics*, *2*(2), 531–543. https://doi.org/10.5194/esurf-2-531-2014
Tsubaki, R., Baranya, S., Muste, M., & Toda, Y. (2018). Spatio-temporal patterns of sediment particle movement on 2D and 3D bedforms. *Experiments in Fluids*, *59*(6), 1–14. https://doi.org/10.1007/s00348-018-2551-y
Tsubaki, R., Kawahara, Y., Muto, Y., & Fujita, I. (2012). New 3-D flow interpolation method on moving ADCP data. *Water Resources Research*, *48*(5), W05539. https://doi.org/10.1029/2011WR010867
Van der Mark, C. F., Blom, A., & Hulscher, S. J. M. H. (2008). Quantification of variability in bedform geometry. *Journal of Geophysical Research*, *113*(F3), F03020. https://doi.org/10.1029/2007JF000940

Van Rijn, L. C. (1984). Sediment transport, part III: Bed forms. *Hydraulic Engineering*, *110*(12), 1733–1754. https://doi.org/10.1061/(ASCE)0733-9429(1984)110:12(1733)

Vericat, D., Wheaton, J. M., & Brasington, J. (2017). Revisiting the morphological approach: Opportunities and challenges with repeat high-resolution topography. In D. Tsutsumi & J. B. Laronne (Eds.), *Gravel-bed rivers: Processes and disasters* (pp. 121–158). Wiley. https://doi.org/10.1002/9781118971437.ch5

Wilbers, A. W. E. (2004). The development and hydraulic roughness of subaqueous dunes (Doctoral dissertation). Utrecht University.

Wilbers, A. W. E., & Ten Brinke, W. B. M. (2003). The response of subaqueous dunes to floods in sand and gravel bed reaches of the Dutch Rhine. *Sedimentology*, *50*(6), 1013–1034. https://doi.org/10.1046/j.1365-3091.2003.00585.x

Wilcock, P. R. (1997). Entrainment, displacement and transport of tracer gravels. *Earth Surface Processes and Landforms: The Journal of the British Geomorphological Research Group*, *22*(12), 1125–1138. https://doi.org/10.1002/(SICI)1096-9837(199712)22:12<1125::AID-ESP811>3.0.CO;2-V

Wu, W., & Wang, S. S. (2006). Formulas for sediment porosity and settling velocity. *Journal of Hydraulic Engineering*, *132*(8), 858–862. https://doi.org/10.1061/(ASCE)0733-9429(2006)132:8(858)

Yalin, M. S. (1964). Geometrical properties of sand wave. *Journal of the Hydraulics Division*, *90*(5), 105–119. https://doi.org/10.1061/JYCEAJ.0001097

Yalin, S. (1964). On the average velocity of flow over a movable bed. *La Houille Blanche*, *50*(1), 45–51. https://doi.org/10.1051/lhb/1964004

You, H. (2023). Data for: On the capabilities of emerging nonintrusive methods to estimate bedform characteristics and bedload rates (Version 1) [Dataset]. Mendley. https://doi.org/10.17632/b7hnj58k5r.1

You, H., Kim, D., & Muste, M. (2021). High-gradient pattern image velocimetry (HGPIV) [Software]. Advances in Water Resources, *159*, 104092. https://doi.org/10.1016/j.advwatres.2021.104092

You, H., Muste, M., Kim, D., & Baranya, S. (2021). Considerations on acoustic mapping velocimetry (AMV) application for in-situ measurement of bedform dynamics. *Frontiers in Water*, *140*, 715308. https://doi.org/10.3389/frwa.2021.715308

Zomer, J. Y., Naqshband, S., & Hoitink, A. J. (2022). A tool for determining multiscale bedform characteristics from bed elevation data. *Earth Surface Dynamics*, *10*(5), 865–874. https://doi.org/10.5194/esurf-10-865-2022